STRONG-COUPLING EFFECTIVE ACTION(S) FOR SU(3) YANG–MILLS*

Stefano Lottini, Owe Philipsen

Institut für Theoretische Physik, Goethe-Universität Frankfurt
Max-von-Laue-Str. 1, 60438 Frankfurt am Main, Germany

Jens Langelage

Fakultät für Physik, Universität Bielefeld
Universitätsstr. 25, 33501 Bielefeld, Germany

(Received July 27, 2011)

We apply strong-coupling expansion techniques to finite-temperature lattice pure gauge theory, obtaining dimensionally reduced Z_N-symmetric effective theories. The analytic mappings between the effective couplings and the original one, *viz.* β, allows to estimate the transition point β_{c} of the 4D theory for a large range of the imaginary-time extent N_τ of the lattice. We study the models for SU(3) via Monte Carlo simulation, finding satisfactory agreement with the critical point of the original theories especially at low N_τ.

DOI:10.5506/APhysPolBSupp.4.721
PACS numbers: 11.15.Ha, 12.38.Aw

1. Introduction and theoretical setting

Among the possible approaches to the study of Lattice QCD, effective theories play an important role, sometimes opening the way to subjects otherwise inaccessible, giving a deeper understanding of the physics at play, or even simply reducing the computational efforts involved. A desirable condition is that the effective theory is motivated by first principles and retains the original symmetries. The history of QCD effective theories is rather long; this work aims at providing the final results for the strong-coupling approach presented in [1].

---

* Presented at the Workshop "Excited QCD 2011", Les Houches, France, February 20–25, 2011.

The effective theories considered in this work re-express the partition function of a $(3+1)$-dimensional Yang–Mills SU(N) lattice theory (all explicit calculations refer to $N=3$) as a three-dimensional model with complex numbers as per-site degrees of freedom, the (traced) Polyakov loops in the 4D system $L_x \equiv \mathrm{Tr}\prod_{\tau=1}^{N_\tau} U_0(x,\tau)$

$$Z = \int [dU] \exp\left(\frac{\beta}{N}\sum_{\Box}\mathrm{ReTr}U_{\Box}\right) \;\Rightarrow\; \int [dL_x] e^{(\lambda_1 S_1[L]+\lambda_2 S_2[L]+\ldots)} . \quad (1)$$

The effective models will exhibit various spin-like interaction terms S_n, each with a specific coupling λ_n which is a function of the imaginary-time extent N_τ of the 4D lattice and its (bare) coupling β. The strong-coupling series for the $\lambda_n(\beta, N_\tau)$ employs a character expansion and then the moment-cumulant formalism [1, 2]; here we only report the final formulae.

Of the (infinitely many) interaction terms, we consider the three featuring the lowest order in β (or in $u \equiv a_f(\beta) \simeq \beta/18 + \mathcal{O}(\beta^2)$, see *e.g.* [2]) nearest- and next-to-nearest-neighbour fundamental representation ($\lambda_1 S_1$, $\lambda_2 S_2$), and nearest-neighbour adjoint interaction ($\lambda_\mathrm{a} S_\mathrm{a}$). We study three different effective theories: one with only the λ_1 interaction, one with (λ_1, λ_2), and the last with the $(\lambda_1, \lambda_\mathrm{a})$ terms. We parametrise L as[1]

$$L_x(\theta_x, \phi_x) = e^{i\theta} + e^{i\phi} + e^{-i(\theta+\phi)} , \qquad -\pi \le \theta_x, \phi_x \le +\pi , \quad (2)$$

$$\int_{\mathrm{SU}(3)} dW_x \mapsto \int_{-\pi}^{+\pi} d\theta_x \int_{-\pi}^{+\pi} d\phi_x \underbrace{\left(27 - 18|L_x|^2 + 8\mathrm{Re}L_x^3 - |L_x|^4\right)}_{\equiv \exp(V_x)} . \quad (3)$$

The effective theories studied numerically are given by[2] $Z_{(1)} \equiv Z_{(1,2)}|_{\lambda_2=0}$,

$$\begin{aligned} Z_{(1,2)} &= \prod_x \int d\theta_x \int d\phi_x \prod_x \exp(V_x) \prod_{\langle i,j\rangle} \left(1 + 2\lambda_1 \mathrm{Re} L_i L_j^*\right) \\ &\quad \prod_{[k,l]} \left(1 + 2\lambda_2 \mathrm{Re} L_k L_l^*\right) , \\ Z_{(1,a)} &= \prod_x \int d\theta_x \int d\phi_x \prod_x \exp(V_x) \prod_{\langle i,j\rangle} \left(1 + 2\lambda_1 \mathrm{Re} L_i L_j^*\right) \\ &\quad \prod_{\langle m,n\rangle} \left[1 + \lambda_a \left(|L_m|^2 - 1\right)\left(|L_n|^2 - 1\right)\right] . \end{aligned} \quad (4)$$

[1] We note that the measure used in [1] contains an error corrected here.
[2] $\langle i,j\rangle$ denotes nearest-neighbours and $[k,l]$ next-to-nearest-neighbours.

In [1] we presented the mappings $\lambda_n \leftrightarrow \beta$ for even N_τ; here we provide in addition $N_\tau = 1, 3$: $\lambda_1(u;1) = u$, $\lambda_2(u;1) = 0$ and $\lambda_a(u;1) = v$; for $N_\tau = 3$ the λ_a map follows the general formula, while

$$\begin{aligned}\lambda_1(u;3) &= u^3 \exp\left[3\left(4u^4+12u^5-14u^6-36u^7+\tfrac{287}{2}u^8+\tfrac{1851}{10}u^9+\tfrac{932917}{5120}u^{10}\right)\right] ,\\ \lambda_2(u;3) &= u^6\left(6u^2+18u^4+117u^6\right) . \end{aligned} \tag{5}$$

2. Numerical simulations and phase structure

All three models were simulated on cubic systems with N_s^3 sites and periodic boundary conditions via a Metropolis accept/reject procedure. Looking at the expressions in Eq. (4), one realises that at sufficiently high couplings a "sign problem" might occur for negative values of $\mathrm{Re}(L_i L_j^*)$: to take care of this, the simulations uses weights $|(1+2\lambda_1 \mathrm{Re} L_i L_j^*)|$ (and similarly for the other terms) and folds the sign into the observable, which is subsequently reweighted to get the correct answer. It turns out that, within the range of couplings of interest, this problem is very mild and the average sign of a configuration never drops below 0.999.

One-coupling model. A first inspection of the distribution of L_x at different couplings confirms the existence of a phase transition at some finite $\lambda_{1,\mathrm{c}}^{(1)}$ (Fig. 1). More quantitatively, we use as basic observable

$$|L| \equiv \frac{1}{N_s^3}\sum_x |L_x| \ . \tag{6}$$

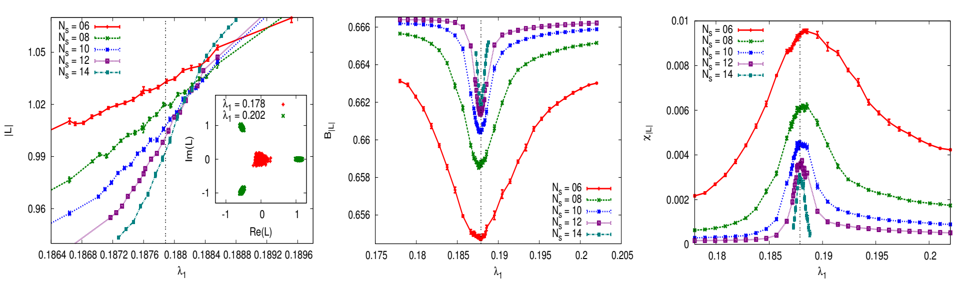

Fig. 1. One-coupling model for various system sizes. Left: behaviour of $|L|$ as a function of λ_1 and (inset) scatter plot of L_x for a small and a large coupling. Middle: Binder cumulant $B_{|L|}$. Right: Susceptibility $\chi_{|L|}$. The vertical line marks the phase transition.

We measure the Binder cumulant and the susceptibility

$$B_{|L|} = 1 - \frac{1}{3}\frac{\langle |L|^4\rangle}{\langle |L|^2\rangle^2} , \qquad \chi_{|L|} = \langle |L|^2\rangle - \langle |L|\rangle^2 , \tag{7}$$

the minimum of the former and the maximum of the latter (see Fig. 1) are used as size-dependent criticality estimators $\lambda_{B,\chi}(N_s)$, and a finite-size scaling fit is then attempted on both, with first-order scaling law

$$\lambda(N_s) = \lambda_{1,c}^{(1)} + bN_s^{-3}\,. \tag{8}$$

Data from systems of side $N_s = 6, 8, 10, 12, 14$ allowed for two independent and consistent estimates of the infinite-volume critical point, averaged to $\lambda_{1,c}^{(1)} = 0.187885(30)$. Further evidence in support of the first-order nature of the transition comes from the scaling of the y-coordinates of the extrema of the observables in Eq. 7: we found for both (Fig. 2)

$$y_{\chi,B}(N_s) = y_{\chi,B}^{\infty} + (\text{const.}) \times N_s^{-3}\,, \tag{9}$$

with $y_\chi^\infty > 0$ and $y_B^\infty = 0.66277(7)$: the latter, as required, is lower than $2/3$, and consistent with the estimate $y_{B,\infty}^* = 0.6617(15)$ coming from locating the two maxima $|L|_{1,2}$ in the distribution of $|L|$ at criticality [3].

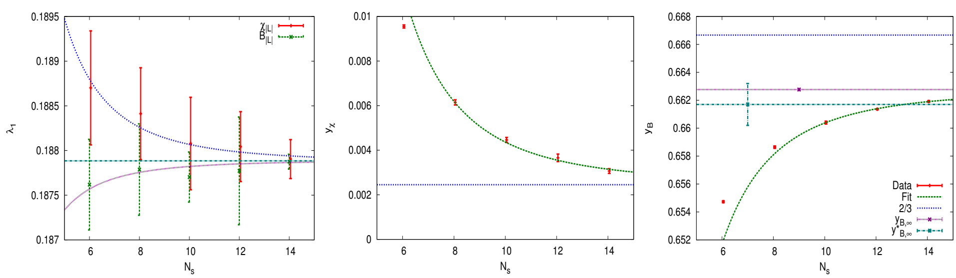

Fig. 2. Scaling analysis for the one-coupling model. Left: data and fit to Eq. (8) for the two pseudo-criticality estimators. Middle: data and fit to Eq. (9). Right: data and fit to Eq. (9), with both estimates for the asymptotic values shown as horizontal lines.

Two-coupling model (λ_1, λ_2). In the two-parameter cases, the β_c of the original gauge theory is found by intersecting the critical line of the models *per se* and one-dimensional manifolds encoding the original theory at N_τ. Ten values of $\lambda_2 \leq 0.01$ were fixed and the approach of the previous case was applied to all of them: a polynomial fit to $\lambda_1 = a_0 + a_1\lambda_2 + a_2\lambda_2^2$ gives the curve in Fig. 3, compatible with the value for $\lambda_2 = 0$, with $a_i = \{0.18787(2), -3.375(8), 12.8(7)\}$.

Two-coupling model (λ_1, λ_a). The same procedure led to a parametrisation of the critical line in the (λ_1, λ_a) plane, with 13 sampled values of $\lambda_a \leq 0.12$. In this case the fitted function was $\lambda_1 = c_0 + c_1\lambda_a + c_2\lambda_a^2 + c_3\lambda_a^3$ (Fig. 3), with coefficients $c_i = \{0.18783(8), -0.50(2), -6.9(7), 30.4(5.7)\}$.

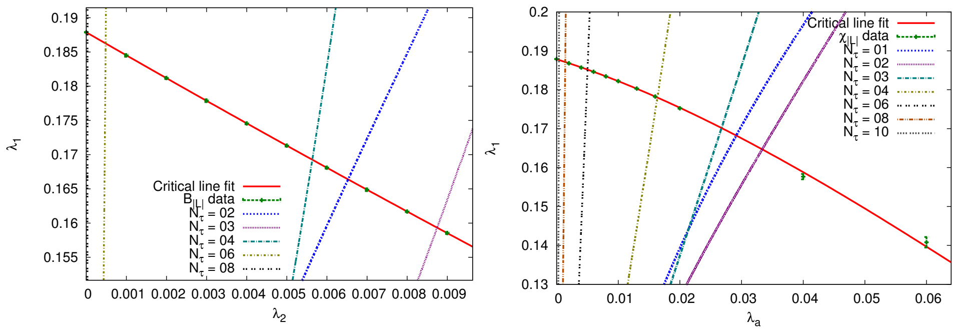

Fig. 3. Two-coupling phase spaces: the critical line parametrisation is shown along with the measured datapoints and the N_τ-specific manifolds, for the $(1,2)$ and $(1,a)$ models (resp. left and right).

3. Results and conclusions

The 4D data were taken from [4, 5], except the $N_\tau = 1$ critical point which was determined with a dedicated set of standard SU(3) Wilson action simulations. The values for $\beta_\mathrm{c}(N_\tau)$ are summarised in Table I and plotted in Fig. 4, along with a plot of the ratio between the effective-theory result and the full 4D Yang–Mills outcome.

TABLE I

Critical couplings for various N_τ from different effective theories compared to the 4D Monte Carlo results.

N_τ	$\beta_\mathrm{c}^{\text{Monte Carlo}}$	$\beta_\mathrm{c}^{(1)}$	$\beta_\mathrm{c}^{(1,2)}$	$\beta_\mathrm{c}^{(1,a)}$
1	2.7030(040)	2.78283(38)	—	2.52906(613)
2	5.1000(500)	5.18391(21)	5.01735(36)	5.00295(513)
3	5.5500(100)	5.84878(11)	5.73325(27)	5.78014(181)
4	5.6925(002)	6.09871(07)	6.05229(11)	6.07479(056)
6	5.8941(005)	6.32625(04)	6.32399(03)	6.32250(011)
8	6.0010(250)	6.43045(03)	6.43033(02)	6.42971(007)
10	6.1600(070)	6.49010(02)	6.49008(02)	6.48991(006)
12	6.2680(120)	6.52875(02)	6.52874(01)	6.52869(005)
14	6.3830(100)	6.55584(02)	6.55583(01)	6.55580(004)
16	6.4500(500)	6.57588(01)	6.57587(01)	6.57585(003)

The discrepancy never exceeds $\sim$ 7–8%; it is noteworthy that the one-coupling action seems to provide the best estimates at $N_\tau = 1, 2$. At low N_τ, where β is smaller, we expect the series expansion to show a better convergence; on the other hand, the particular shape of the mappings $\lambda_i(\beta)$ is such that, as N_τ increases, only the λ_1 coupling is important, which is the reason why the various results tend to converge one onto another.

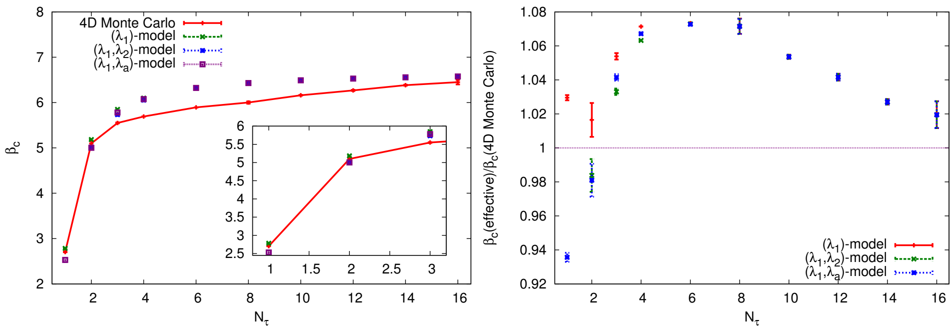

Fig. 4. Comparison between the determinations of $\beta_c(N_\tau)$ from the effective models and the 4D Monte Carlo results. Left: plot of β_c. Right: the ratio $\beta_c^{\rm eff}/\beta_c^{\rm Monte\ Carlo}$.

It must be stressed that the present results, able to reproduce the critical points with some accuracy, are obtained with a rather small computational effort (3D instead of 4D and complex numbers instead of matrices), measurable in the range of a few days with an ordinary desktop PC. This is in contrast with the "inverse Monte Carlo" approach [6], which requires simulating the full theory in order to fix the coefficients; on the other hand, the latter technique is able to reproduce the theory on both sides of the transition.

An extension of the present work is currently being carried on, with the introduction of massive fermions in the effective formulation via a hopping-parameter expansion.

REFERENCES

[1] J. Langelage, S. Lottini, O. Philipsen, *J. High Energy Phys.* **1102**, 057 (2011) [`arXiv:arXiv:1010.0951v2 [hep-lat]`].

[2] I. Montvay, G. Münster, *Quantum Fields on a Lattice, Cambridge Monographs on Mathematical Physics*, Cambridge Univ. Press, UK, 1994, p. 491.

[3] J. Lee, J.M. Kosterlitz, *Phys. Rev.* **B43**, 3265 (1991).

[4] J. Kogut, M. Stone, H.W. Wyld, *Phys. Rev. Lett.* **50**, 393 (1983).

[5] J. Fingberg, U.M. Heller, F. Karsch, *Nucl. Phys.* **B392**, 493 (1993).

[6] C. Wozar, T. Kaestner, A. Wipf, T. Heinzl, *Phys. Rev.* **D76**, 085004 (2007) [`arXiv:0704.2570v1 [hep-lat]`].